




Unexpected dose response of HaCaT to UVB irradiation

Rong-Shing Chang¹ · Chi-Shuo Chen¹ · Ching-Lung Huang¹ · Chiu-Ting Chang¹ · Yujia Cui¹ · Wei-Ju Chung · Wun-Yi Shu² · Chi-Shiun Chiang¹ · Chun-Yu Chuang¹ · Ian C. Hsu¹ 

Received: 10 May 2018 / Accepted: 12 July 2018 / Editor: Tetsuji Okamoto
© The Society for In Vitro Biology 2018

Abstract

Application of high-dosage UVB irradiation in phototherapeutic dermatological treatments present health concerns attributed to UV-exposure. In assessing UV-induced photobiological damage, we investigated dose-dependent effects of UVB irradiation on human keratinocyte cells (HaCaT). Our study implemented survival and apoptosis assays and revealed an unexpected dose response wherein higher UVB-dosage induced higher viability. Established inhibitors, such as AKT– (LY294002), PKC– (Gö6976, and Rottlerin), ERK– (PD98059), P38 MAPK– (SB203580), and JNK– (SP600125), were assessed to investigate UV-induced apoptotic pathways. Despite unobvious contributions of known signaling pathways in dose-response mediation, microarray analysis identified transcriptional expression of UVB-response genes related to the respiratory-chain. Observed correlation of ROS-production with UVB irradiation potentiated ROS as the underlying mechanism for observed dose responses. Inability of established pathways to explain such responses suggests the complex nature underlying UVB-phototherapy response.

Keywords Proliferation · Apoptosis · UVB, ultraviolet B · Phototherapy · ROS, reactive oxygen species

Introduction

UVB phototherapy is a common treatment for skin disorders (Lee et al. 2005; Jo et al. 2011; Mehta and Lim 2016), such as atopic dermatitis and psoriasis. Efficacy of such treatment has been verified clinically, but looming concern regarding risks of UV light-induced skin cancers have been debated across decades. A MEDLINE-search study suggested risk of skin cancer is not significantly increased with UVB phototherapy (Lee et al. 2005). In addition to the study for Caucasian population, the retrospective study conducted in Asia indicated that the UVB phototherapy seems to be a safe therapeutic modality for patients (Jo et al. 2011). Conversely, a disparate investigation suggested that UV exposure may not only cause erythema and immunosuppression but also lead to photo-aging and photo-carcinogenesis (Matsumura and Ananthaswamy 2004). High correlation between cancer

suppressor protein p53 and apoptosis regulation in psoriasis patients was found in immunostaining results of psoriasis skin biopsies (Moorchung et al. 2015). Moreover, it was widely demonstrated that UV exposure can either stimulate the p53 expression (Henseleit et al. 1997; Qin et al. 2002) which implies the potential DNA damage (Schürer et al. 1993; Herzinger et al. 1995; Takasawa et al. 2005; Aitken et al. 2007). Since p53 mutations were identified in psoriasis patients, relevant studies have been conducted investigating the mutations caused by UV-based phototherapy (Nataraj et al. 1997; Seidl et al. 2001; Mudigonda et al. 2012). As a sequential treatment with replicative UV irradiation, phototherapy potentiates photo-carcinogenesis in affected tissues. Considering close association between the mutated p53 and psoriasis, we implemented HaCaT as our model in evaluating the UVB response of p53-mutant keratinocytes.

Genetic regulation pathways, protein phosphorylation kinase, and protein/chromophore/nuclear acid metabolisms have been accessed to investigate mediation of UVB-induced cellular responses (Lewis et al. 2003; Assefa et al. 2005; Van Laethem et al. 2009). For instance, membrane survival/apoptosis-related pathways, such as PKB/AKT (Decraene et al. 2002; Gonzales and Bowden 2002), PKC (Denning et al. 1998; Efimova et al. 2004), p38 MAPK (Chen et al. 1999; Peus et al. 1999), ERK (Peus et al. 1999), and JNK (Tourmier et al. 2000; Bivik and Ollinger 2008); are involved in cellular

✉ Ian C. Hsu
ichsu@mx.nthu.edu.tw

¹ Department of Biomedical Engineering and Environmental Sciences, National Tsing Hua University, 101, Section2, Kuang-Fu Road, Hsinchu 30013, Taiwan

² Institute of Statistics, National Tsing Hua University, Hsinchu, Taiwan

responses to UVB in various cell types. In addition, molecular mechanisms underlying apoptosis have been studied (Lotti et al. 2007; Lee et al. 2013). Various models can be delineated from intracellular chromophores to the attendant reactive oxygen species (ROS) (Kulms and Schwarz 2002; Heck et al. 2003; Assefa et al. 2005; Van Laethem et al. 2009; Ryu et al. 2010; Lee et al. 2017). The ROS induced by exogenous agents is produced by chromophores after absorbing UV rays (Adler et al. 1999; Ding et al. 2002), while ROS induced by endogenous agents are stimulated by cellular stress response pathways following UV irradiation (Kulms and Schwarz 2002). Growing evidence suggests that the endogenous agent-derived ROS perpetuates from mitochondria (Chance et al. 1979; Cadenas and Davies 2000), whereby serving as a signaling molecule in the apoptotic pathway.

Studies reported the differences of cell response according to UV irradiation dosage (Gentile et al. 2003; Shimmura et al. 2004). Mammone et al. reported that HaCaT cells underwent apoptosis and necrosis under UVB irradiation dosage of 50–200 J/m² or > 200 J/m², respectively (Mammone et al. 2000). Using UV-irradiated HaCaT cells, Takasawa et al. confirmed the differences in the caspase activation pathway between UVB- and UVC-induced apoptosis at 100–500-J/m² UVB or 30–150-J/m² UVC, respectively. In addition, higher UVB dose (1000–4000 J/m²) is applied in cellular apoptosis and phototherapy-related studies (Takeuchi et al. 2004; Lee et al. 2005; Knezevic et al. 2007; Nakamura et al. 2016). Such results suggest that onset of disparate pathways depends on UV irradiation dosage. In assessing the potential influences of UVB phototherapy, our study implemented a UVB dosage range from 100 to 1000 J/m², corresponding to accepted dosing guidelines from American Academy of Dermatology (Mudigonda et al. 2012).

Materials and Methods

Cells and cell culture Human keratinocyte cell line (HaCaT), obtained from Dr. Norbert Fusening (German Cancer Research Center, Heidelberg, Germany), is a spontaneously transformed human epithelial cell line (Boukamp et al. 1988) carrying mutated p53 at both alleles (Lehman et al. 1993). HaCaT cells reflect well the characteristics of primary cultured skin keratinocytes *in vitro* (Boukamp et al. 1988) and were grown in Dulbecco's modified Eagle's medium (Gibco-BRL, Grand Island, NY) supplemented with 1× penicillin-streptomycin-glutamine (Gibco-BRL) and 10% fetal bovine serum (HyClone, Logan, UT). All cultures were maintained at 37°C in a humidified atmosphere with 5% CO₂.

UVB irradiation Light source was a 6-W UVB lamp assembled with a EN-160 filter (Spectronics, Westbury, NY). UVB

dosage was measured with an IL-1400A radiometer (International light, Newburyport, MA), equipped with a wide band UV detector (SED005/WBS320/W, International light, and the coefficient of variation (C.V.) of intensities in the 55-cm² illumination field was 2.15%. Before cells were exposed to UVB radiation, cells were rinsed twice with prewarmed PBS. HaCaT cells were then irradiated with 233 (low dose) or 582.5 (high dose) J/m² (dose rate 3.88 W/m²) UVB in 10-cm uncovered dishes (Corning, Rochester, NY) with a thin layer of PBS. PBS was removed immediately after UVB irradiation, and cells were replenished with previously collected medium and incubated at 37°C for indicated periods of time prior to RNA extraction. A control set of cells was treated identically at each time period, except for UVB radiation.

Trypan blue exclusion test of cell viability Cell viability was evaluated in terms of cell membrane integrity using trypan blue (Sigma, St. Louis, MO) exclusion assay. At scheduled time periods, cells were collected with 1.5 ml of 0.25-mM trypsin and 0.53-mM EDTA (Gibco-BRL), then were suspended by gentle pipetting. Viable cells were identified by trypan blue exclusion assay with a hemocytometer. Results were presented as a ratio of treated cells to the number of control cells.

MTT assay The mitochondrial activity of HaCaT cell treated with UVB was evaluated using the 3-(4,5-dimethylthiazol-2-yl)-2,5-diphenyltetrazolium bromide (Sigma) conversion method. Four hours before harvesting, cells were incubated with 0.33-mg/ml MTT; the cells were then lysed with 4 ml of dimethyl sulfoxide (Calbiochem, Darmstadt, Germany) to dissolve the formazan. The relative reduction activities were presented as the ratio of absorbance of the treatment cells to that of the control cells.

Time-lapse microscopy The culture dish was placed on an inverted microscope, which was enclosed in an incubator at 37°C and 5% CO₂. A shutter was used to control the illumination light. The frequency of image acquisition was set to 1 s⁻¹.

Cell cycle analysis by propidium iodide Analysis of cell cycle profile was performed 8 and 16 h after UVB exposure. Experiment was conducted following a standard flow cytometry protocol. In brief, cells were harvested, washed twice with PBS, fixed with 70% ethanol, and incubated with 1-mg/ml RNase A (Sigma Aldrich) for 30 min at 37°C and then stained with PI (1 mg/ml; Molecular Probes) for 30 min at 37°C. The cell cycle profile was measured using a flow cytometer, CyFlow (Partec, Münster, Germany). A typical run used for one sample contained 20,000 counts.

Selective pathway inhibitor The classic PKC inhibitor, Gö6976; the c-Jun N-terminal kinase-specific inhibitor, SP600125; the p38 kinase inhibitor, SB203580; the p42/44 mitogen-activated protein (MAP) kinase cascade inhibitor, PD98059; the PI-3 kinase inhibitor, LY294002; or the protein kinase C (PKC)- δ inhibitor, Rottlerin was respectively added in culture medium 2 h prior to UVB exposure. In addition, DMSO, which is the solvent used for all the inhibitors mentioned above, was used for vehicle control. Cell viability was estimated by MTT assay 24 h after UVB irradiation.

Microarray transcriptomic profiling At each indicated time period, cells were washed twice with PBS and lysed directly in the culture dish with 2-ml TRIzol reagent (Invitrogen, Carlsbad, CA). Total RNA was isolated according to the manufacturer's protocol and purified with RNeasy Mini kit (Qiagen, Valencia, CA) resulting in A260/A280 ratios of 1.9–2.1. RNA quality was examined by Agilent 2100 bioanalyzer and the RNA 6000 Nano Assay kit (Agilent, Palo Alto, CA).

Each RNA sample was labeled by an indirect method using the 3DNA Array 50 kit (Genisphere, Hatfield, PA). Briefly, 20- μ g total RNA was used to perform reverse transcription reaction with SuperScript II RNase H-reverse transcriptase and specific primers (Invitrogen, Carlsbad, CA). Then all synthesized tagged cDNA targets were purified by Microcon YM-30 column (Millipore, Billerica, MA). The purified targets and fluorescent 3DNA reagents were hybridized to the arrays in succession. Hybridization was performed at 65°C, in a water bath for 20 h, and arrays were washed according to the manufacturer protocol. Subsequently, arrays were scanned with GenePix 4000B (Axon, Union City, CA), and images were acquired by GenePix Pro 3.0 software. More detail about the manufacture of microarray as well as the loop-design experiments and analysis, please see our previous publication (Tsai et al. 2009).

ROS detection H2DCFDA (2',7'-dichlorodihydrofluorescein diacetate) was used as probes for ROS detected in HaCaT cells. To load the probe, cells dissociated with trypsin were followed by a 10-min incubation with 20-mM H2DCFDA in the dark at 37°C. Intracellular ROS was quantified by the intensity of H2DCFDA in the cells irradiated with UVB before loading the probe 30 min in advance. The intensity of the fluorophore was measured by CyFlow flow cytometer (Partec, Münster, Germany). For each sample, 10,000 ungated events were acquired.

Annexin V apoptosis assay Analysis of annexin V binding was conducted with an Annexin V-FITC Detection Kit I (BD Bioscience, San Diego, CA). After trypsinization, cells were collected, washed twice with cold phosphate-buffered saline,

and centrifuged at 1000 r.p.m. for 5 min. Cells were resuspended in $1\times$ binding buffer, which was supplied by the kit, at a concentration of 10^6 cells/ml, 100 μ l of the solution that was transferred to a tube, and 5 μ l of annexin V-FITC and 5 μ l of propidium iodide (PI) were added. Cells were gently vortexed and incubated for 15 min at room temperature in the dark. Before data acquisition, 2 ml of $1\times$ binding buffer was added to each tube, and samples were analyzed by a flow cytometer (Partec). For each sample, 10,000 ungated events were acquired.

Western blots Cells were irradiated with 0 (control), 233 (low dose), or 582.5 (high dose) J/m^2 of UVB and then harvested at the indicated time period after UVB irradiation. Right before harvest, cells were washed with PBS twice and incubated in lysis buffer in the presence of a protease inhibitor cocktail (Epitomics, Burlingame, CA). Protein content was estimated according to the manufacturers' instruction using Bio-Rad protein assay reagent (Bio-Rad, Hercules, CA). Cellular proteins were electrophoresed in a 10% polyacrylamide gel and transferred to a PVDF membrane (Millipore, Billerica, MA) followed by a blocking procedure in blocking buffer (1XTBST, 5% BSA). After washing off the blocking residue by TBST, the blots were incubated with a rabbit monoclonal anti-PARP antibody (Epitomics, Burlingame, CA), as well as with monoclonal anti- β -actin antibody (Santa Cruz Biotechnology) and then washed again. The HRP-linked (horse radish peroxidase) secondary antibody was labeled, and peroxidase activity was detected by ECL chemiluminescence in a film imager (Fuji, Stamford, CT).

Statistical analysis For most of experiments, such as MTT and apoptosis assay, we presented our results with mean SD of triplicate experiments and determined the differences of data with Student's *t* test.

Results

Unexpected dose response and viability of HaCaT cells to UVB irradiation Cellular viability of UVB-exposed HaCaT cells was assessed under UVB irradiation of dose ranged from 0 to $1165 J/m^2$. All cells were examined by MTT assay and trypan blue viability assay (Fig. 1a) at 24 h after UVB irradiation. We observed an unusual dose response within the dose range of 233 (low dose) to $582.5 J/m^2$ (high dose). Within that range, cellular survival rates were higher relative to cells treated with higher doses. Surviving fractions of HaCaT cells were further examined by MTT assay at specific time points after UV irradiation (Fig. 1b). Results showed that surviving fractions of low-dose-treated cells seemed lower than surviving fractions of high-dose-treated

cells at 16 h after UVB treatment (low dose 0.32 ± 0.02887 , high dose 0.4133 ± 0.0348 , p value = 0.1079), and there is significant difference (low dose 0.17 ± 0.001 ; high dose 0.41 ± 0.0046 , p value = 0.0073) between surviving fractions of different dose treatments at 24 h after UVB treatment.

Dynamic cell morphology was monitored by time-lapsed microscopy, whereby differences between cells under low- versus high-dose treatments were subtle 12 h after irradiation. However, four additional hours revealed cells treated with low-dosage had a significantly higher proportion of apoptotic cells relative to the high-dosage group (Fig. 1c).

Apoptosis of HaCaT induced by various UVB doses To further substantiate the occurrence of apoptosis, we performed an annexin V apoptosis assay. Results indicated that 20.9 and 11.2% of low- and high-dose irradiated cells underwent apoptosis 10 h following treatment, respectively (Fig. 2a). Moreover, our data revealed increasing percentage of the apoptosis in cells treated with UVB doses lower than the Low

dose, and these results revealed that there exists a dose-dependent apoptotic response both in early and late apoptotic stages when HaCaT cells were irradiated with UVB doses lower than the low-dose (Fig. 2b).

The halting cell cycle progression by UVB irradiation In monitoring cell morphology with time-lapse microscopy, cell mitosis ceased following UVB irradiation of both low-dose and high-dose. To monitor the cell cycle progression after UVB irradiation, we implemented the cell cycle analysis assay with PI (Fig. 2c). At 8 h time point, there was 31% of cells in subG1 phase with low-dose exposure, comparing to 20 (control) and 17% (high-dose). Similar phenomenon was observed at 16 h; the subG1 percentage of cell with low dose (36%) is higher than the control group (14%) and the group with high dose (11%).

Such finding suggests that the UVB-irradiated cells halt cell cycle progression due to the absence of mitosis. In addition, the greater population of subG1 phase of the low-dose sample was found than that of the high-dose sample at 8 and 16 h.

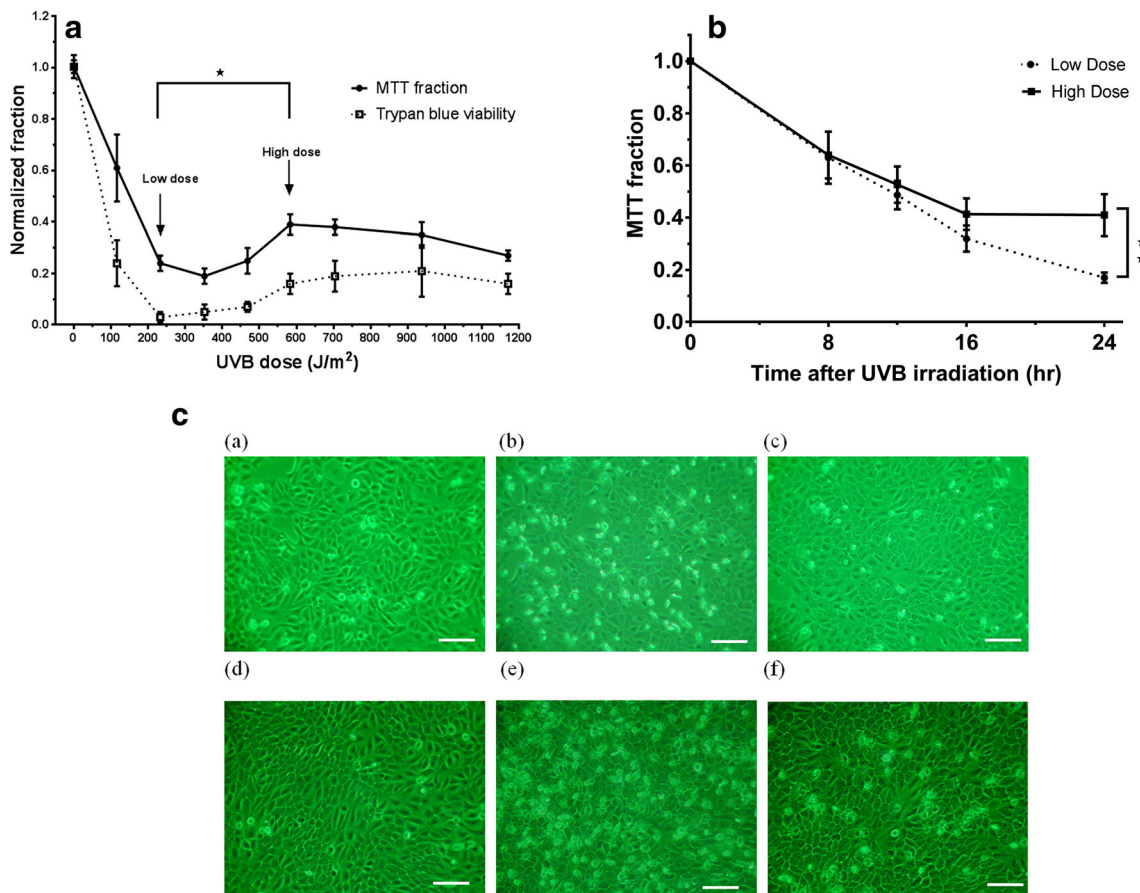


Figure 1. Cellular activity and survival rate. (a) Cellular viability was measured by MTT assay (solid line) and trypan blue viability test (dash line) 24 h after UVB irradiation. An abnormal dose response within the dose range of 233 (low dose) to 582.5 (high dose) J/m² can be observed in both MTT and trypan blue assay. (b) Cells exposed to low-dose UVB

radiation after 16 h post-UVB treatment had lower survival rate than cells exposed to high-dose UVB radiation did. The error bar represents mean \pm SD of triplicate experiments. (c) Time-lapse microscopy images of cells exposed to low-dose UVB and high-dose UVB.

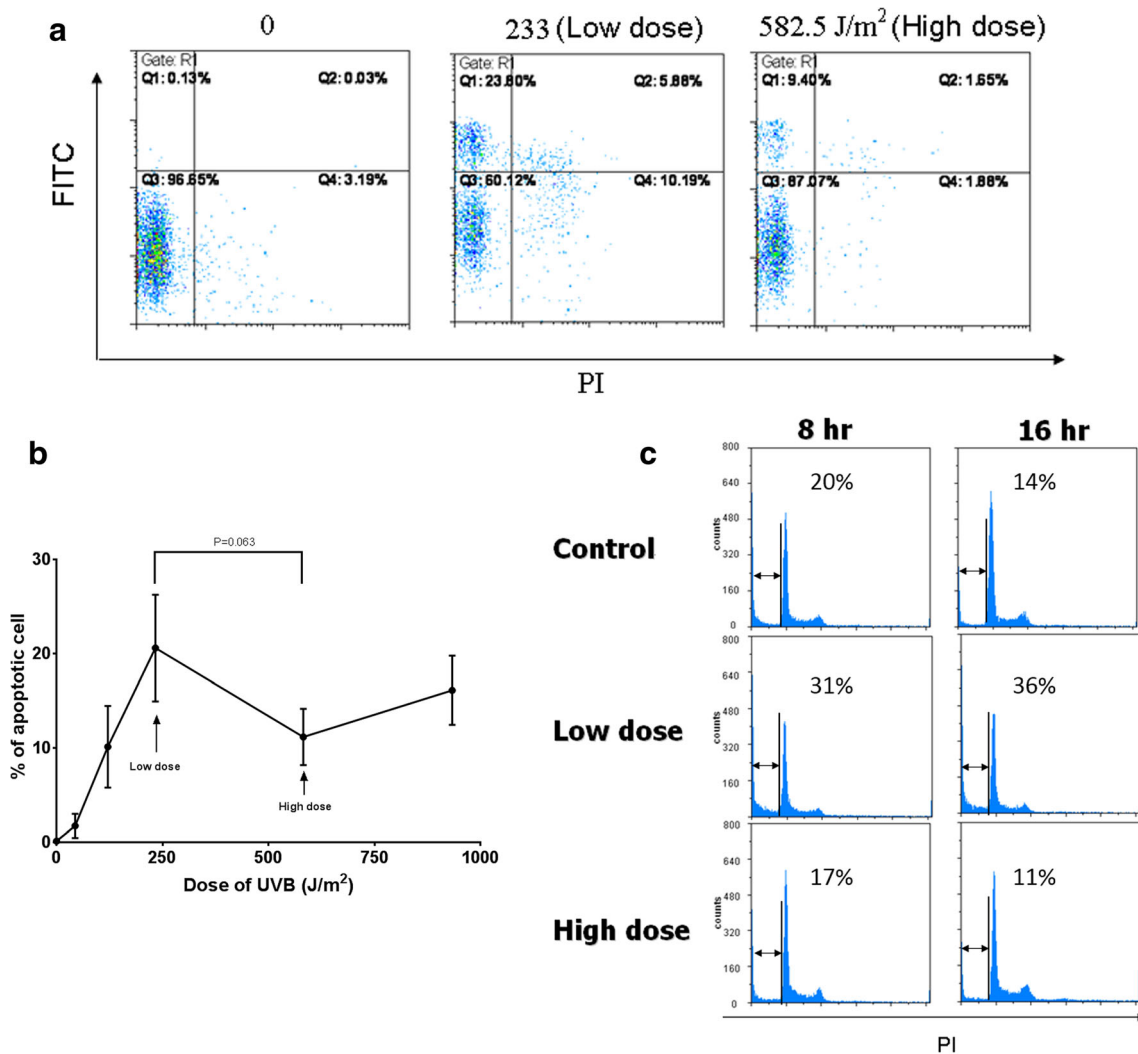


Figure 2. Flow cytometry analysis of UVB irradiated HaCaT. (a) The dot plot analysis of annexin V apoptosis assay with our triplicate experiments. (b) The quantitative results of annexin V apoptosis assay. Percent of apoptotic cells are calculated as the summation of PI positive quadrant

and annexin V positive quadrant. The *error bar* represents mean \pm SD of triplicate samples. (c) Cell cycle analysis of UVB irradiated HaCaT cells. The cells were exposed to low-dose and high-dose UVB, and then processed with cell cycle analysis assay at indicated time periods.

Monotonic dose-dependent response in transcriptional level

To obtain a global view of the gene expression involved in this unusual dose-response phenomenon, we performed a microarray study with loop-designed experiments and analyses (Fig. 3a) (Tsai et al. 2009). The data are available at the Gene Expression Omnibus database (<http://www.ncbi.nlm.nih.gov/geo/>) under the GSE series accession number GSE4223. Gene expression ratios of low-dose UVB-treated cells over their corresponding control sample are dotted in ascending order (in blue) and those of high-dose UVB-treated cells are then plotted in an identical gene order (in red) (Fig. 3b). At earlier times (0.5, 1, and 2 h), genes of low- (in blue) and high-dose (in red) UVB-irradiated HaCaT cells expressed in a dose dependent manner as if the UVB effects are additive in the level of RNA expression. However, this additive phenomenon

became inconspicuous later. Results show that most of the differentially expressed genes exhibited dose dependency, especially at earlier times. However, more discordantly expressed genes, as well as inverse dose-response genes, were found at later time points.

Transcriptional up-regulation of respiratory chain-related genes

In evaluating the influence of oxidative phosphorylation, 19 genes related to the respiratory chain reaction were selected from our 7334 microarray-identified genes following irradiation. In this work, those 19 genes were also up-regulated after UVB irradiation in HaCaT cell (Fig. 4a) In response to low-dose treatment, five genes related to the respiratory chain reaction were differentially up-regulated (two genes in complex I: NDUFA9, NDUFB7; one in complex III: QP-C; two in complex

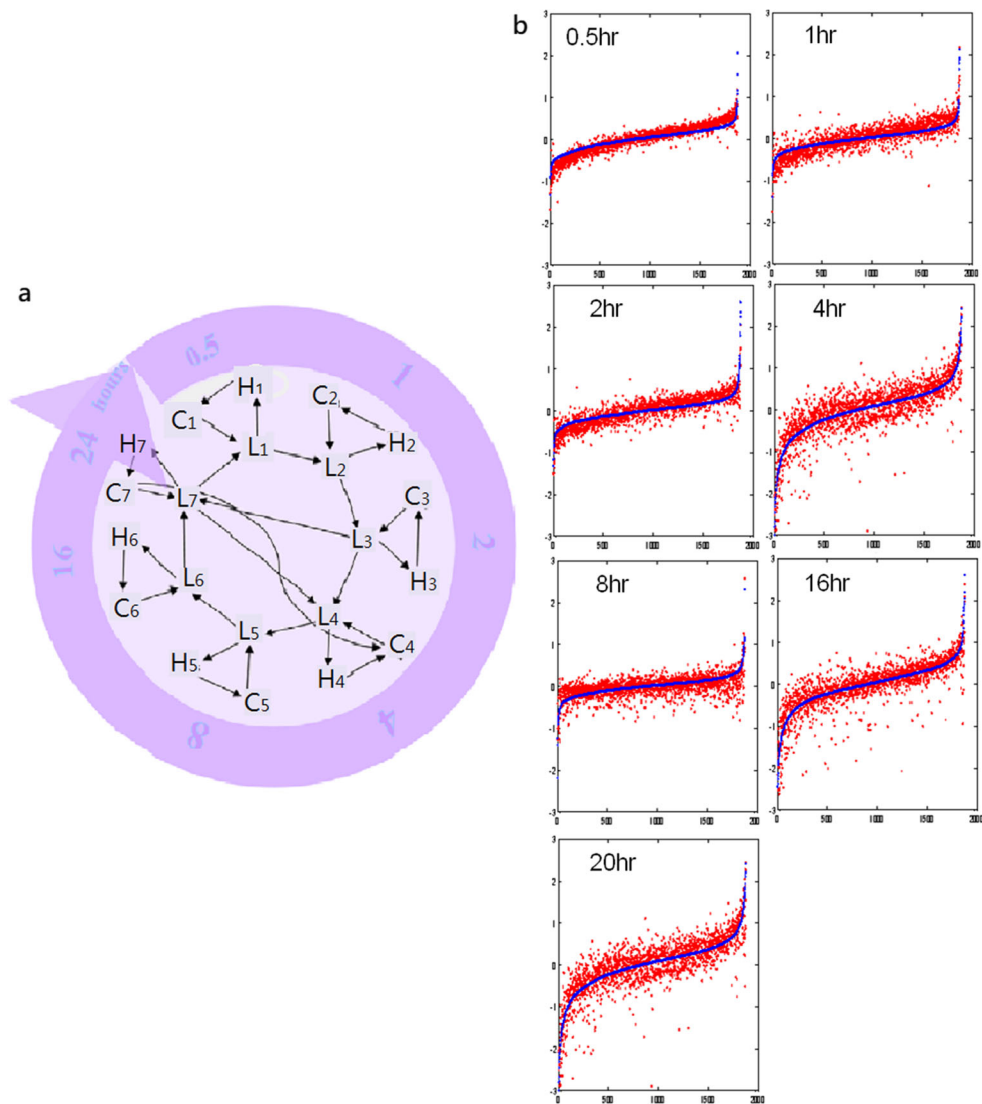


Figure 3. Transcriptional gene express profile of low- and high-dose UVB irradiated cells. (a) Microarray loop design. Samples appear at the tail/head of each arrow are labeled with Cy3/Cy5. The symbols “Ci/Li/Hi” denote the samples of control/low-dose UVB-irradiated/high-dose

UVB-irradiated cells harvested at each time period (*i* from 1 to 7 indicating 0.5, 1, 2, 4, 8, 16, 20 h), after UVB exposure. (b) The gene expression of low (in blue) and high (in red) over their corresponding control sample are dotted in ascending order.

IV: COX5A and COX10). In response to high-dose treatment, 18 genes involved in the respiratory chain reaction (nine genes in respiratory chain complex I; three in complexes III, IV, and V) were found differentially up-regulated. The expression profiles of all these genes were depicted for both low- and high-dose UVB irradiation (Fig. 4b, c).

ROS productions associated with the unexpected dose response Levels of intracellular ROS were assessed in HaCaT cells treated with or without UVB using ROS-sensitive probe *H2DCFDA*. Results showed elevated intracellular ROS following low-dose or high-dose UVB irradiation (Fig. 5a), where the intracellular ROS level is

an important index to evaluate the damages led by UVB exposure. The results consist with previous studies, which demonstrated that intracellular ROS levels were significantly elevated after UVB irradiation (Kulms and Schwarz 2002; Ryu et al. 2010).

Results highlighted general dose-dependency of respiratory electron transport chain associated genes at earlier time-points (Fig. 4). Seventeen out of 19 dose-dependent respiratory chain related genes up-regulated.

To reaffirm the influence of ROS, we applied ROS scavenger *Diphenylene iodonium (DPI)*, wherein cells were pre-incubated with 2- μ M DPI for 1 h before exposure to UVB. MTT assays were then performed at 20 h after UVB irradiation. Results show diminishment of the unexpected dose-

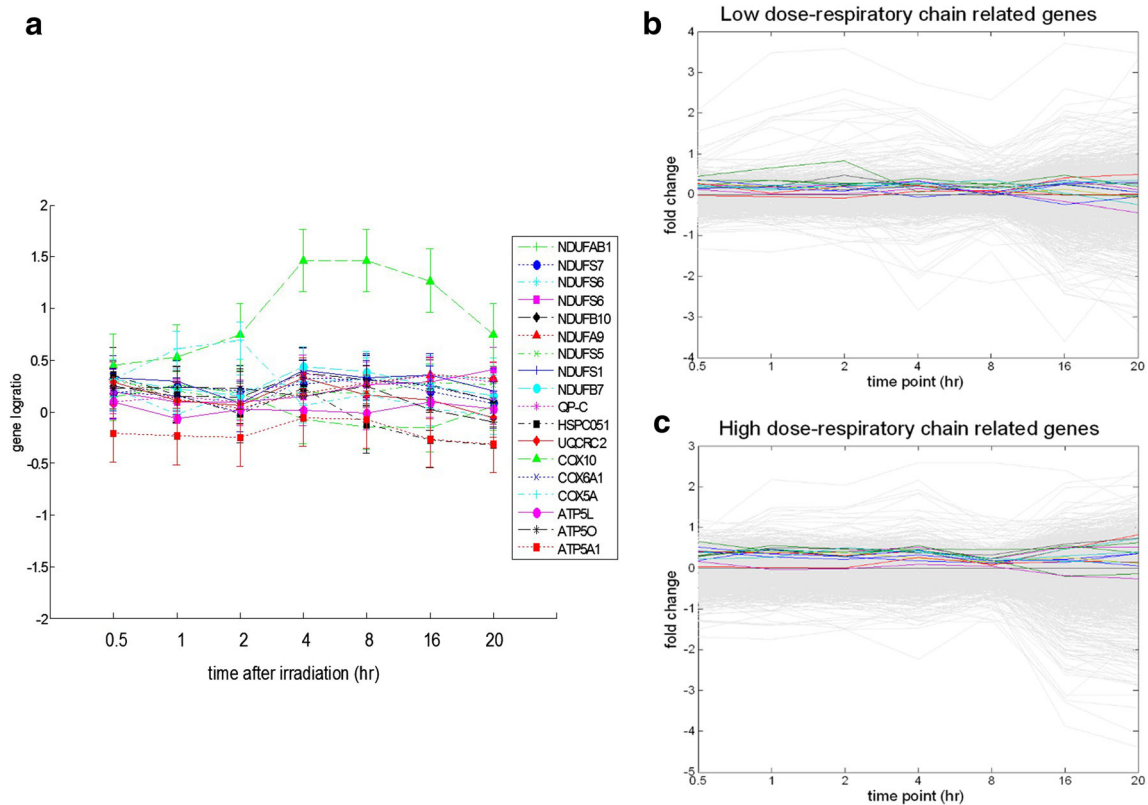


Figure 4. The expression of respiratory chain related genes. The expression fold change is the ratio of gene expression of UVB irradiated sample over the corresponding control sample. (a) Selected mitochondrial respiratory chain genes. (b) Gene expression fold change

(log₂ ratio) of low-dose UVB treated HaCaT cells. (c) Gene expression fold change (log₂ ratio) of high-dose UVB treated HaCaT cells. All genes that passed the quality control criteria are plotted in gray, while respiratory chain related genes are identified in color.

response phenomenon with DPI pre-incubation. Cells pre-incubated with 2- μ M DPI exhibited lower ability of MTT reduction after high-dose relative to low dose UVB irradiation (Fig. 5b).

DPI, which abolished the unexpected dose response in this study, was previously reported to inhibit the activity of NOX (O'Donnell et al. 1993) and NOS (Stuehr et al. 1991). We consequently measured activity of these two

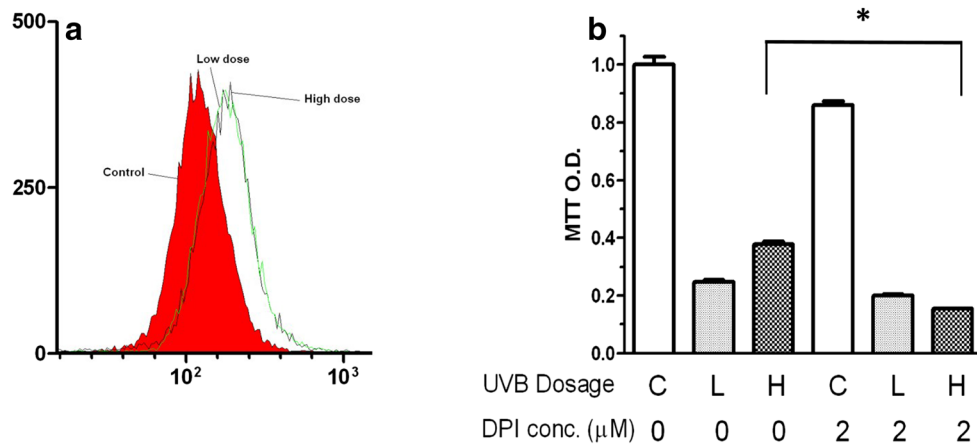


Figure 5. ROS and the abnormal dose response. (a) Elevated intracellular ROS level in HaCaT cells 30 min after UVB irradiation. Representative histograms of triplicate experiments plot the relative green DCF fluorescence intensity. The results of flow cytometry contain 10,000 ungated events. (b) DPI rectifies the abnormal dose response of UVB

irradiated HaCaT cells. HaCaT cells pretreated with DPI were irradiated with indicated dose of UVB and then MTT assay were conducted 24 h after UVB irradiation. The data was normalized to control sample without DPI pretreatment.

enzymes with or without pretreatment of DPI. Without pretreatment, NBT assay revealed higher levels of NOX activity in HaCaT cells UVB-irradiated at higher levels relative to non-treated groups (Fig. 6). With pretreatment, HaCaT cells exhibit lower levels of NOX activity following UVB irradiation. Furthermore, the Griess assay demonstrated an extremely low level (close to the detection limit) of NOS in the culture medium and, thus, suggested no involvement of NOS in cell-response to UVB irradiation (Fig. 7).

Effect of selective pathway inhibitors Previous studies revealed that UVB-induced apoptosis occurs via activation of kinase pathways such as PI3K/Akt (protein kinase B) signal transduction, ERK1/2 and p38, and protein kinase C. In order to identify the potential roles of these pathways in the unexpected UVB response observed in this study, HaCaT cells were pretreated with inhibitors which blocked these signal transduction pathways prior to UVB irradiation. Levels of induced apoptosis increased in case of inhibited PI3K/Akt or protein kinase C (Fig. 8). However, cell viability was not significantly altered when cells were pretreated with the other four inhibitors. In order to verify the validity of LY294002, which mostly suppressed the survival among all blockades we assayed, Western blotting experiments were conducted (Fig. 9). AKT was phosphorylated at 0.5 and 2 h after exposure of UVB. However, AKT phosphorylation was inhibited when cells were pretreated with LY294002.

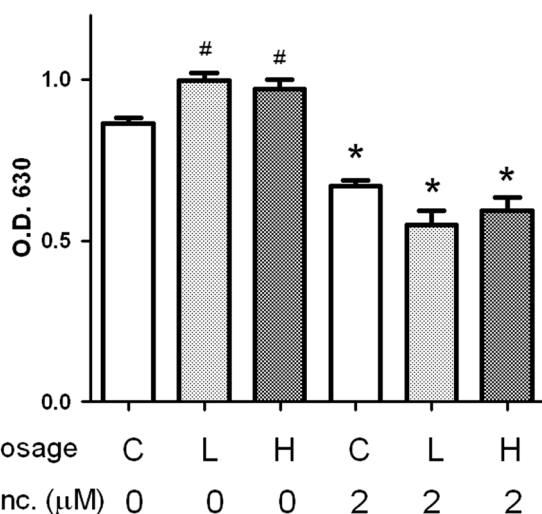


Figure 6. O₂⁻ production of HaCaT cells after UVB irradiation with and without DPI pretreatment. Nitroblue tetrazolium (NBT) reduction assay was used to detect the O₂⁻ production. No significant difference of O₂⁻ between low- and high-dose irradiated cells was detected regardless of DPI pretreatment. (* indicates significance to the corresponding non-DPI-pretreated sample, and # indicates significance to the none-UVB-irradiated sample).

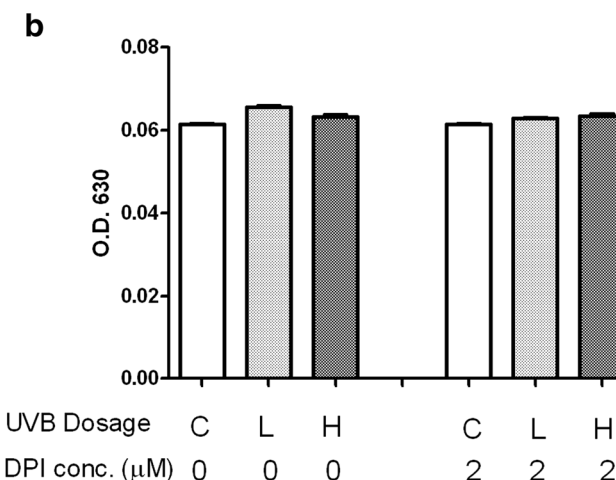
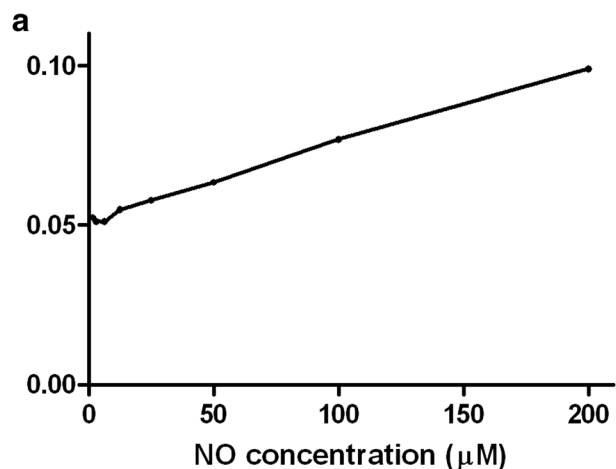


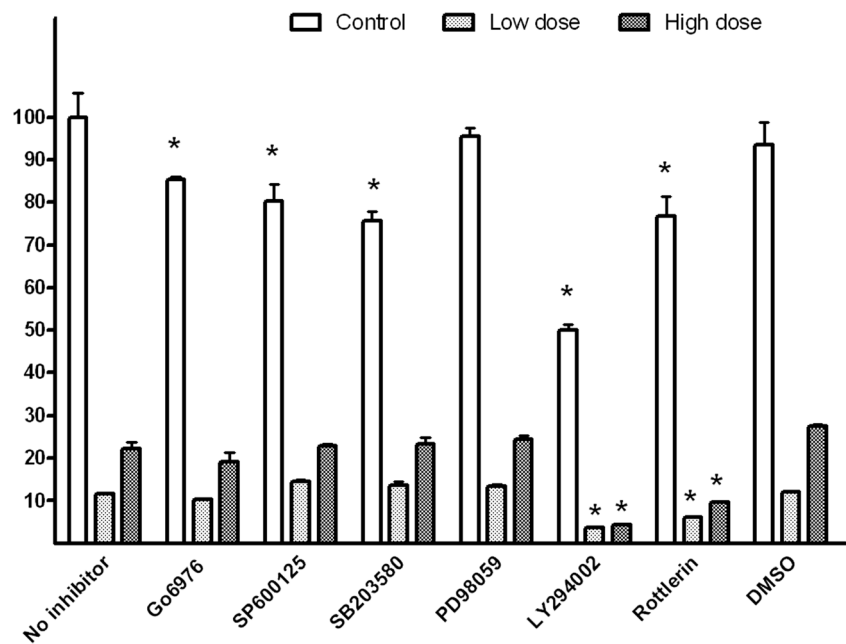
Figure 7. No significant level of nitric oxide production in HaCaT cells after UVB irradiation. Nitric oxide production was measured by the Griess assay. (a) The standard curve was illustrated by serial dilution of NaNO₂ to indicate concentration. (b) The nitric oxide production was as low as the range out the linear standard curve under every experimental condition.

Furthermore, to examine the decreased cell viability caused by LY294002 induced apoptosis, we measured the production of cleaved PARP, which is an early indicator of apoptosis (Fig. 10). PARP cleavages were found at 2- and 7-h following UVB irradiation in cells that were pretreated with LY294002, while samples without LY294002 pretreatment exhibited an insignificant PARP cleavage. Even so, the unexpected dose response remained. Low-dose irradiated HaCaT cells carried more cleaved PARP than high-dose irradiated HaCaT cells did.

Discussion

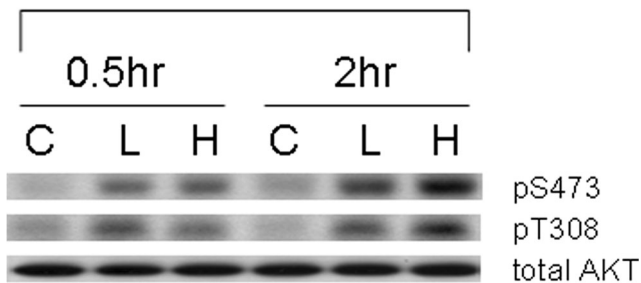
In this study, we utilized several assays to confirm the dose response and viability of HaCaT cells to UVB irradiation. Both MTT and annexin V apoptosis assays showed lower cell

Figure 8. Rottlerin and LY294002 reduce cellular activity but do not alter the abnormal dose response to UVB. Cellular activity of HaCaT cells was evaluated by the MTT assay at 24 h after low- or high-dose UVB irradiation pretreated with indicated selective pathway inhibitor. Rottlerin and LY294002 pretreatments reduce the cellular activity after both low- and high-dose UVB irradiation.



survival rate under low irradiation dosage, while higher subG1 proportion was found in low-dosage-treated cells. Our current

a w/o LY294002



b w/ LY294002

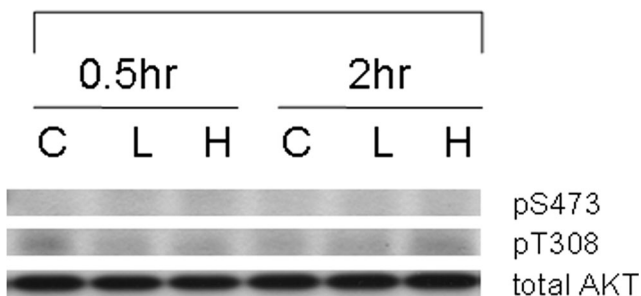


Figure 9. PI3K/AKT provoked by UVB and inhibited by LY294002. (a) AKT is phosphorylated after both low- and high-dose of UVB irradiation whether at the site S473 or T308. (b) AKT phosphorylation was inhibited by LY294002 even with UVB irradiation.

findings reveal an unexpected dose response of HaCaT cells to UVB radiation. Different from the previous study (Takasawa et al. 2005), the surviving fraction of cells was inversely proportional to UVB exposure in the dosage range between 233 and 582.5 J/m². In order to explore the underlying mechanism, various well-known signaling pathways were evaluated in our microarray system (Tsai et al. 2009). Our microarray data reveal a transcriptional UVB-activation expression of respiratory chain related genes, and the result demonstrated an additive effect of RNA expression to UVB irradiation of HaCaT cells only at earlier times, although transient gene expression may have prolonged effects at all monitored times. Moreover, several previous studies suggested disparate doses of UV irradiation may encourage cells to undergo various pathways (Mammone et al. 2000; Latonen et al. 2001; Gentile et al. 2003; Shimmura et al. 2004), but this irregular response phenomenon has yet to be reported. Gentile et al. reported that UVC irradiation induced transcriptionally and highly distinct responses in human fibroblast (Gentile et al. 2003). In our study, microarray data illustrated the diminishment of gene expression alteration with time. Although many microarray analyses of UV damage responses have been conducted (Becker et al. 2001; Sesto et al. 2002; Gentile et al. 2003), few have identified the transient perturbation on gene expression. The up-regulation of respiration chain related genes was concurrent with our previous study of UVB-irradiated human fibroblast (MRC5) microarray experiment (Tsai et al. 2009). Thus, we further investigated the close correlation between ROS production and the unexpected UVB response. Our current experimental setting, H2DCFDA probing assay, revealed that levels of intracellular ROS in UVB-irradiated cells were

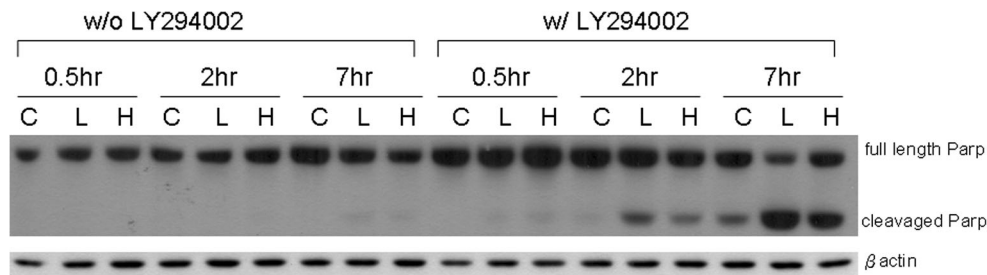


Figure 10. Enhancement of Parp cleavage by pretreating LY294002 (an inhibitor of AKT) after UVB irradiation. HaCaT cells were pretreated with or without LY294002 before indicated dose of UVB irradiation (C,

L, and H). After UVB irradiation, cells were harvested at indicated time period and lysates were subjected to Western blot analysis using anti-PARP antibody.

significantly elevated without dose dependency. This inconsistency of early responsive gene expression and consequent ROS production potentially provides a mechanism, which mediate the unexpected dose response of HaCaT cells to UVB irradiation. In addition, ROS scavenger DPI was found to diminish the unexpected dose response, which suggested suppressive effects of DPI on NOX activity. Though it cannot be conclusive proof that NOX dominates the unexpected dose-dependent phenomenon, DPI represents progress toward identifying the mechanism which characterizes the unexpected dose response of HaCaT to UVB irradiation.

In this study, we applied six selective pathway inhibitors to detect kinase-pathway involvement, and inhibitors, Rottlerin and LY294002, suppressed survival of UVB-irradiated HaCaT cells. Considering persistence of the unexpected dose response, the involvement of the six explored pathways is unlikely.

Conclusions

Considering mutated p53 is closely associated with psoriasis and skin cancer, we implemented HaCaT as our model cell line to study UVB response. In this study, findings revealed an unexpected dose response of HaCaT cells to UVB irradiation.

Though our study has not identified specific mechanisms for this response phenomenon, evidence potentiates involvement of ROS in this phenomenon. These results not only highlight the significance of ROS interaction but also imply the complexity of UVB-phototherapy treatment.

Funding information The work was supported by grants from the Ministry of Science and Technology, Taiwan (MOST 104-2112-M-007-016). C.S.C was supported by the Ministry of Science and Technology, Taiwan (MOST 105-2112-M-007-010).

References

Adler V, Yin Z, Tew KD, Ronai Z (1999) Role of redox potential and reactive oxygen species in stress signaling. *Oncogene* 18:6104–6111

- Aitken GR, Henderson JR, Chang SC, McNeil CJ, Birch-Machin MA (2007) Direct monitoring of UV-induced free radical generation in HaCaT keratinocytes. *Clin Exp Dermatol* 32:722–727
- Assefa Z, Van Laethem A, Garmyn M, Agostinis P (2005) Ultraviolet radiation-induced apoptosis in keratinocytes: on the role of cytosolic factors. *Biochim Biophys Acta* 1755:90–106
- Becker B, Vogt T, Landthaler M, Stolz W (2001) Detection of differentially regulated genes in keratinocytes by cDNA array hybridization: Hsp27 and other novel players in response to artificial ultraviolet radiation. *J Invest Dermatol* 116:983–988
- Bivik C, Ollinger K (2008) JNK mediates UVB-induced apoptosis upstream lysosomal membrane permeabilization and Bcl-2 family proteins. *Apoptosis* 13:1111–1120
- Boukamp P, Petrussevska RT, Breitkreutz D, Hornung J, Markham A, Fusenig NE (1988) Normal keratinization in a spontaneously immortalized aneuploid human keratinocyte cell line. *J Cell Biol* 106:761–771
- Cadenas E, Davies KJ (2000) Mitochondrial free radical generation, oxidative stress, and aging. *Free Radic Biol Med* 29:222–230
- Chance B, Sies H, Boveris A (1979) Hydroperoxide metabolism in mammalian organs. *Physiol Rev* 59:527–605
- Chen N, Ma W, Huang C, Dong Z (1999) Translocation of protein kinase Cepsilon and protein kinase Cdelta to membrane is required for ultraviolet B-induced activation of mitogen-activated protein kinases and apoptosis. *J Biol Chem* 274:15389–15394
- Decraene D, Agostinis P, Bouillon R, Degreef H, Garmyn M (2002) Insulin-like growth factor-1-mediated AKT activation postpones the onset of ultraviolet B-induced apoptosis, providing more time for cyclobutane thymine dimer removal in primary human keratinocytes. *J Biol Chem* 277:32587–32595
- Denning MF, Wang Y, Nickoloff BJ, Wrona-Smith T (1998) Protein kinase Cdelta is activated by caspase-dependent proteolysis during ultraviolet radiation-induced apoptosis of human keratinocytes. *J Biol Chem* 273:29995–30002
- Ding M, Li J, Leonard SS, Shi X, Costa M, Castranova V, Vallyathan V, Huang C (2002) Differential role of hydrogen peroxide in UV-induced signal transduction. *Mol Cell Biochem* 234–235:81–90
- Efimova T, Broome AM, Eckert RL (2004) Protein kinase Cdelta regulates keratinocyte death and survival by regulating activity and subcellular localization of a p38delta-extracellular signal-regulated kinase 1/2 complex. *Mol Cell Biol* 24:8167–8183
- Gentile M, Latonen L, Laiho M (2003) Cell cycle arrest and apoptosis provoked by UV radiation-induced DNA damage are transcriptionally highly divergent responses. *Nucleic Acids Res* 31:4779–4790
- Gonzales M, Bowden GT (2002) The role of PI 3-kinase in the UVB-induced expression of c-fos. *Oncogene* 21:2721–2728
- Heck DE, Vetrano AM, Mariano TM, Laskin JD (2003) UVB light stimulates production of reactive oxygen species unexpected role for catalase. *J Biol Chem* 278:22432–22436

- Henseleit U, Zhang J, Wanner R, Haase I, Kolde G, Rosenbach T (1997) Role of p53 in UVB-induced apoptosis in human HaCaT keratinocytes. *J Invest Dermatol* 109:722–727
- Herzinger T, Funk JO, Hillmer K, Eick D, Wolf DA, Kind P (1995) Ultraviolet B irradiation-induced G2 cell cycle arrest in human keratinocytes by inhibitory phosphorylation of the cdc2 cell cycle kinase. *Oncogene* 11:2151–2156
- Jo SJ, Kwon HH, Choi MR, Youn JI (2011) No evidence for increased skin cancer risk in Koreans with skin phototypes III–V treated with narrowband UVB phototherapy. *Acta Derm-Venereol* 91:40–43
- Knezevic D, Zhang W, Rochette PJ, Brash DE (2007) Bcl-2 is the target of a UV-inducible apoptosis switch and a node for UV signaling. *P Natl Acad Sci USA* 104:11286–11291
- Kulms D, Schwarz T (2002) Independent contribution of three different pathways to ultraviolet-B-induced apoptosis. *Biochem Pharmacol* 64:837–841
- Latonen L, Taya Y, Laiho M (2001) UV-radiation induces dose-dependent regulation of p53 response and modulates p53-HDM2 interaction in human fibroblasts. *Oncogene* 20:6784–6793
- Lee C-H, Wu S-B, Hong C-H, Yu H-S, Wei Y-H (2013) Molecular mechanisms of UV-induced apoptosis and its effects on skin residential cells: the implication in UV-based phototherapy. *Int J Mol Sci* 14: 6414–6435
- Lee E, Bae H, Lee H, Jang Y, Park YH, Kim J, Ryu WI, Choi B, Kim J, Jeong S (2017) Intracellular ROS levels determine the apoptotic potential of keratinocyte by quantum dot via blockade of AKT phosphorylation. *Exp Dermatol* 26:1046–1052
- Lee E, Koo J, Berger T (2005) UVB phototherapy and skin cancer risk: a review of the literature. *Int J Dermatol* 44:355–360
- Lehman TA, Modali R, Boukamp P, Stanek J, Bennett WP, Welsh JA, Metcalf RA, Stampfer MR, Fusenig N, Rogan EM et al (1993) p53 mutations in human immortalized epithelial cell lines. *Carcinogenesis* 14:833–839
- Lewis DA, Hurwitz SA, Spandau DF (2003) UVB-induced apoptosis in normal human keratinocytes: role of the erbB receptor family. *Exp Cell Res* 284:314–325
- Lotti LV, Rotolo S, Francescangeli F, Frati L, Torrisi MR, Marchese C (2007) AKT and MAPK signaling in KGF-treated and UVB-exposed human epidermal cells. *J Cell Physiol* 212:633–642
- Mammone T, Gan D, Collins D, Lockshin RA, Marenus K, Maes D (2000) Successful separation of apoptosis and necrosis pathways in HaCaT keratinocyte cells induced by UVB irradiation. *Cell Biol Toxicol* 16:293–302
- Matsumura Y, Ananthaswamy HN (2004) Toxic effects of ultraviolet radiation on the skin. *Toxicol Appl Pharm* 195:298–308
- Mehta D, Lim HW (2016) Ultraviolet B phototherapy for psoriasis: review of practical guidelines. *Am J Clin Dermatol* 17:125–133
- Moorchung N, Vasudevan B, Kumar SD, Muralidhar A (2015) Expression of apoptosis regulating proteins p53 and bcl-2 in psoriasis. *Indian J Pathol Microbiol* 58:423–426
- Mudigonda T, Dabade TS, Feldman SR (2012) A review of targeted ultraviolet B phototherapy for psoriasis. *J Am Acad Dermatol* 66: 664–672
- Nakamura M, Farahnik B, Bhutani T (2016) Recent advances in phototherapy for psoriasis. *F1000Res* 5
- Nataraj AJ, Wolf P, Cerroni L, Ananthaswamy HN (1997) p53 mutation in squamous cell carcinomas from psoriasis patients treated with psoralen plus UVA (PUVA). *J Invest Dermatol* 109:238–243
- O'Donnell BV, Tew DG, Jones OT, England PJ (1993) Studies on the inhibitory mechanism of iodonium compounds with special reference to neutrophil NADPH oxidase. *Biochem J* 290(Pt 1):41–49
- Peus D, Vasa RA, Beyerle A, Meves A, Krautmacher C, Pittelkow MR (1999) UVB activates ERK1/2 and p38 signaling pathways via reactive oxygen species in cultured keratinocytes. *J Invest Dermatol* 112:751–756
- Qin JZ, Chaturvedi V, Denning MF, Bacon P, Panella J, Choubey D, Nickoloff BJ (2002) Regulation of apoptosis by p53 in UV-irradiated human epidermis, psoriatic plaques and senescent keratinocytes. *Oncogene* 21:2991–3002
- Ryu HC, Kim C, Kim JY, Chung JH, Kim JH (2010) UVB radiation induces apoptosis in keratinocytes by activating a pathway linked to “BLT2-reactive oxygen species”. *J Invest Dermatol* 130:1095–1106
- Schürer N, Köhne A, Schliep V, Barlag K, Goerz G (1993) Lipid composition and synthesis of HaCaT cells, an immortalized human keratinocyte line, in comparison with normal human adult keratinocytes. *Exp Dermatol* 2:179–185
- Seidl H, Kreimer-Erlacher H, Back B, Soyer HP, Hofler G, Kerl H, Wolf P (2001) Ultraviolet exposure as the main initiator of p53 mutations in basal cell carcinomas from psoralen and ultraviolet A-treated patients with psoriasis. *J Invest Dermatol* 117:365–370
- Sesto A, Navarro M, Burslem F, Jorcano JL (2002) Analysis of the ultraviolet B response in primary human keratinocytes using oligonucleotide microarrays. *Proc Natl Acad Sci U S A* 99:2965–2970
- Shimmura S, Tadano K, Tsubota K (2004) UV dose-dependent caspase activation in a corneal epithelial cell line. *Curr Eye Res* 28:85–92
- Stuehr DJ, Fasehun OA, Kwon NS, Gross SS, Gonzalez JA, Levi R, Nathan CF (1991) Inhibition of macrophage and endothelial cell nitric oxide synthase by diphenyleneiodonium and its analogs. *FASEB J* 5:98–103
- Takasawa R, Nakamura H, Mori T, Tanuma S (2005) Differential apoptotic pathways in human keratinocyte HaCaT cells exposed to UVB and UVC. *Apoptosis* 10:1121–1130
- Takeuchi S, Zhang WG, Wakamatsu K, Ito S, Hearing VJ, Kraemer KH, Brash DE (2004) Melanin acts as a cause an atypical potent UVB photosensitizer to mode of cell death in murine skin. *P Natl Acad Sci USA* 101:15076–15081
- Tournier C, Hess P, Yang DD, Xu J, Turner TK, Nimmual A, Bar-Sagi D, Jones SN, Flavell RA, Davis RJ (2000) Requirement of JNK for stress-induced activation of the cytochrome c-mediated death pathway. *Science* 288:870–874
- Tsai ML, Chang KY, Chiang CS, Shu WY, Weng TC, Chen CR, Huang CL, Lin HK, Hsu IC (2009) UVB radiation induces persistent activation of ribosome and oxidative phosphorylation pathways. *Radiat Res* 171:716–724
- Van Laethem A, Garmyn M, Agostinis P (2009) Starting and propagating apoptotic signals in UVB irradiated keratinocytes. *Photochem Photobiol Sci* 8:299–308